

Supporting information

Tailoring Intraband Transition via Composition in Self-doped $\text{Ag}_2\text{S}_x\text{Se}_y$ Alloy Nanocrystals

Youngjo Choi[†], Haemin Song[‡], Gyu Ho Song[†], Hee Kwon Kim[†], Yoon Seo Jung[‡], Hyeong Seok Kang[‡], Woong Kim^{,†,a} and Kwang Seob Jeong^{*‡}*

[†]Department of Materials Science and Engineering, Korea University, 145 Anam-ro, Seongbuk-gu, Seoul, 02841, Republic of Korea

^aDepartment of Semiconductor System Engineering, Korea University, 145 Anam-ro, Seongbuk-gu, Seoul, 02841, Republic of Korea

[‡]Department of Chemistry, Korea University, 145 Anam-ro, Seongbuk-gu, Seoul, 02841, Republic of Korea

AUTHOR INFORMATION

Corresponding Author

*E-mail: woongkim@korea.ac.kr (W. Kim)

*E-mail: kwangsjeong@korea.ac.kr (K. S. Jeong)

Table of Contents

Fig. S1. The TEM images of the $\text{Ag}_2\text{S}_x\text{Se}_y$ nanocrystals with various sulfur contents: (a) $\text{Ag}_2\text{Se}_{0.75}$, (b) $\text{Ag}_2\text{S}_{0.07}\text{Se}_{0.79}$, (c) $\text{Ag}_2\text{S}_{0.17}\text{Se}_{0.61}$, (d) $\text{Ag}_2\text{S}_{0.67}\text{Se}_{0.15}$, and (e) $\text{Ag}_2\text{S}_{0.81}$ (scale bars = 10 nm).

Table S1. The crystal sizes of the various $\text{Ag}_2\text{S}_x\text{Se}_y$ nanocrystals.

Fig. S2. A photographic image of the $\text{Ag}_2\text{S}_{0.23}\text{Se}_{0.51}$ nanocrystals dispersed in toluene.

Fig. S3. The XPS survey spectra of the various $\text{Ag}_2\text{S}_x\text{Se}_y$ nanocrystals.

Fig. S4. The fitting results of XPS spectra of S 2p and Se 3p region of the various $\text{Ag}_2\text{S}_x\text{Se}_y$ nanocrystals.

Fig. S5. The fitting results of XPS spectra of Ag 3d region of the various $\text{Ag}_2\text{S}_x\text{Se}_y$ nanocrystals.

Table S2. The peak locations of XPS spectra (Se 3p, S 2p, and Ag 3d) of the various $\text{Ag}_2\text{S}_x\text{Se}_y$ nanocrystals.

Fig. S6. The absorption spectra of the $\text{Ag}_2\text{S}_x\text{Se}_y$ nanocrystals fitted with Gaussian curves.

Fig. S7. The trends in the intraband and band gap transitions of the $\text{Ag}_2\text{S}_{0.23}\text{Se}_{0.51}$ nanocrystals at various SEC potentials.

Fig. S8. The differential absorption spectra of (a) the $\text{Ag}_2\text{S}_{0.09}\text{Se}_{0.75}$ and (b) the $\text{Ag}_2\text{S}_{0.23}\text{Se}_{0.62}$ nanocrystals under various electrochemical potentials, as obtained from the SEC measurements.

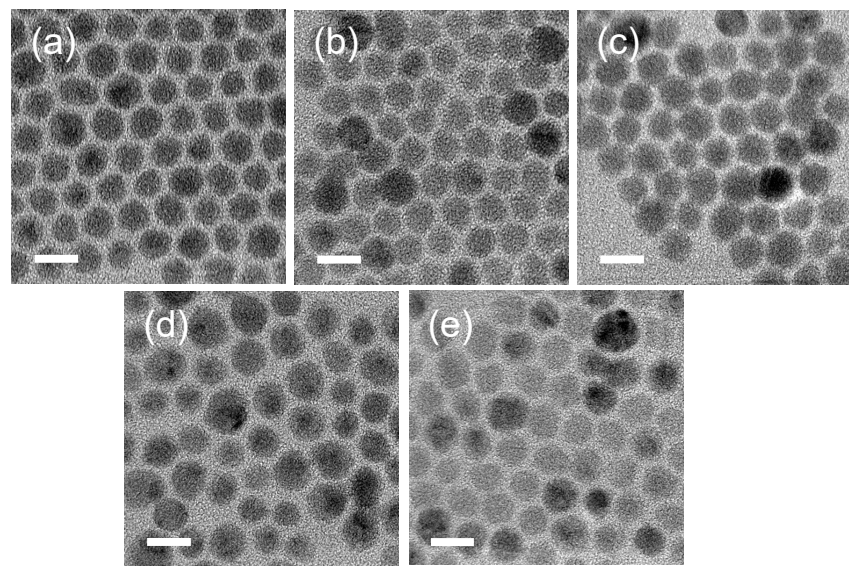


Fig. S1. The TEM images of the $\text{Ag}_2\text{S}_x\text{Se}_y$ nanocrystals with various sulfur contents: (a) $\text{Ag}_2\text{Se}_{0.75}$, (b) $\text{Ag}_2\text{S}_{0.07}\text{Se}_{0.79}$, (c) $\text{Ag}_2\text{S}_{0.17}\text{Se}_{0.61}$, (d) $\text{Ag}_2\text{S}_{0.67}\text{Se}_{0.15}$, and (e) $\text{Ag}_2\text{S}_{0.81}$ (scale bars = 10 nm).

Table S1. The crystal sizes of the various $\text{Ag}_2\text{S}_x\text{Se}_y$ nanocrystals.

	$\text{Ag}_2\text{Se}_{0.75}$	$\text{Ag}_2\text{S}_{0.07}\text{Se}_{0.79}$	$\text{Ag}_2\text{S}_{0.17}\text{Se}_{0.61}$	$\text{Ag}_2\text{S}_{0.24}\text{Se}_{0.49}$	$\text{Ag}_2\text{S}_{0.53}\text{Se}_{0.35}$	$\text{Ag}_2\text{S}_{0.67}\text{Se}_{0.15}$	$\text{Ag}_2\text{S}_{0.81}$
Size (nm)	6.3 ± 0.9	6.2 ± 0.7	6.5 ± 0.8	6.4 ± 0.6	5.9 ± 1.3	6.2 ± 1.1	6.2 ± 0.8

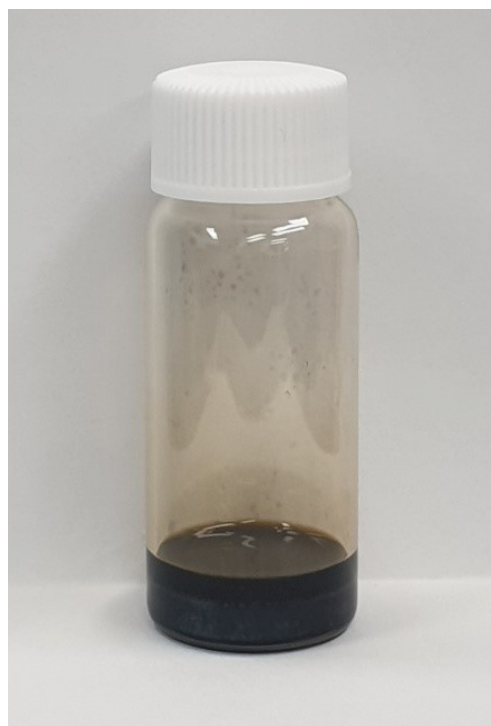


Fig. S2. A photographic image of the $\text{Ag}_2\text{S}_{0.23}\text{Se}_{0.51}$ nanocrystals dispersed in toluene.

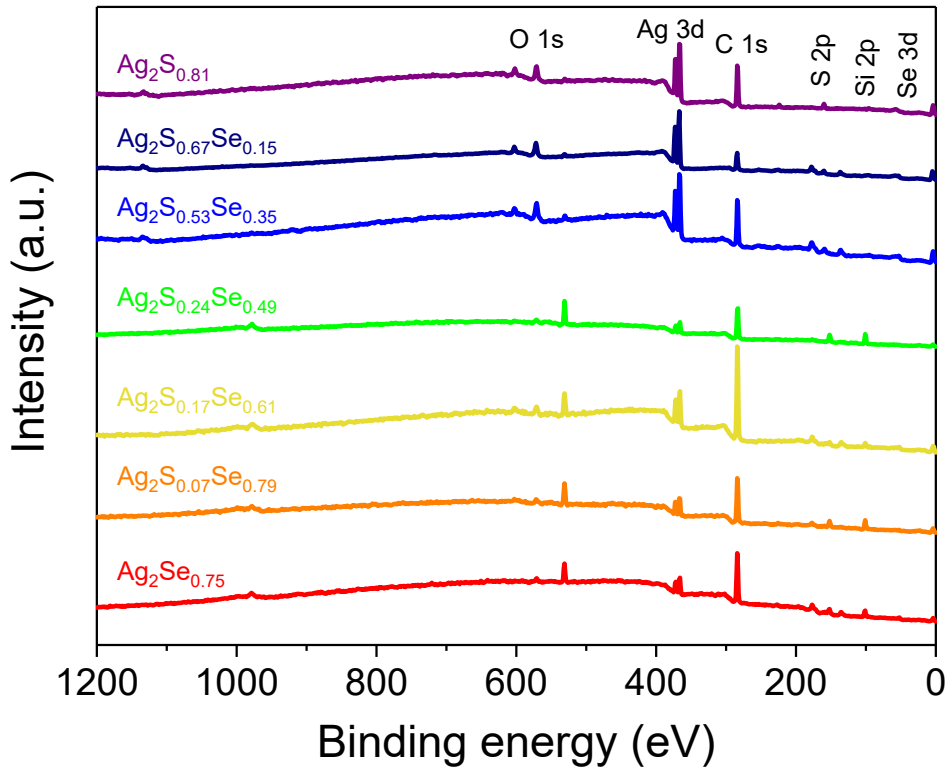


Fig. S3. The XPS survey spectra of the various $\text{Ag}_2\text{S}_x\text{Se}_y$ nanocrystals.

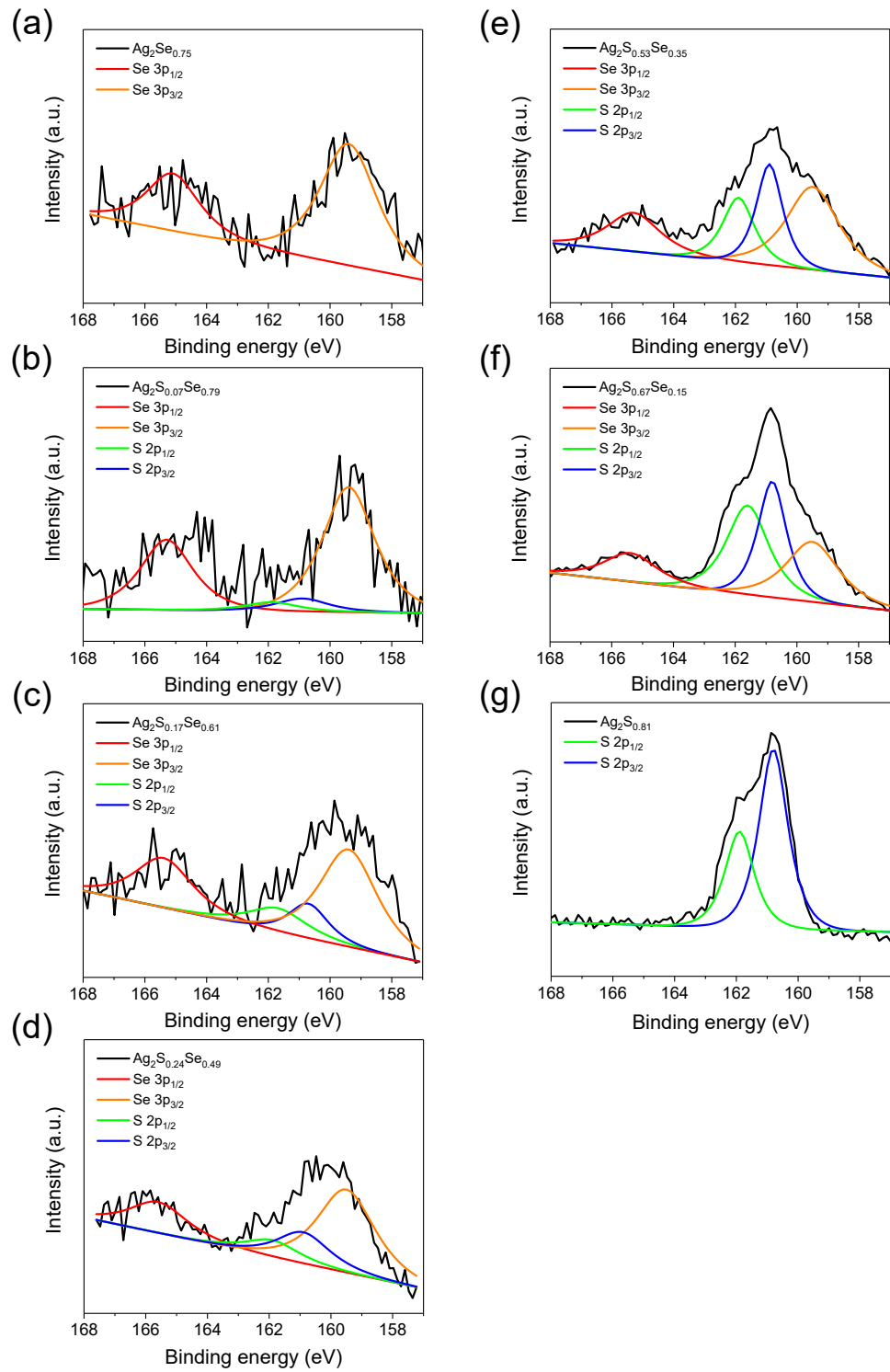


Fig. S4. The fitting results of XPS spectra of S 2p and Se 3p region of the various $\text{Ag}_2\text{S}_x\text{Se}_y$ nanocrystals.

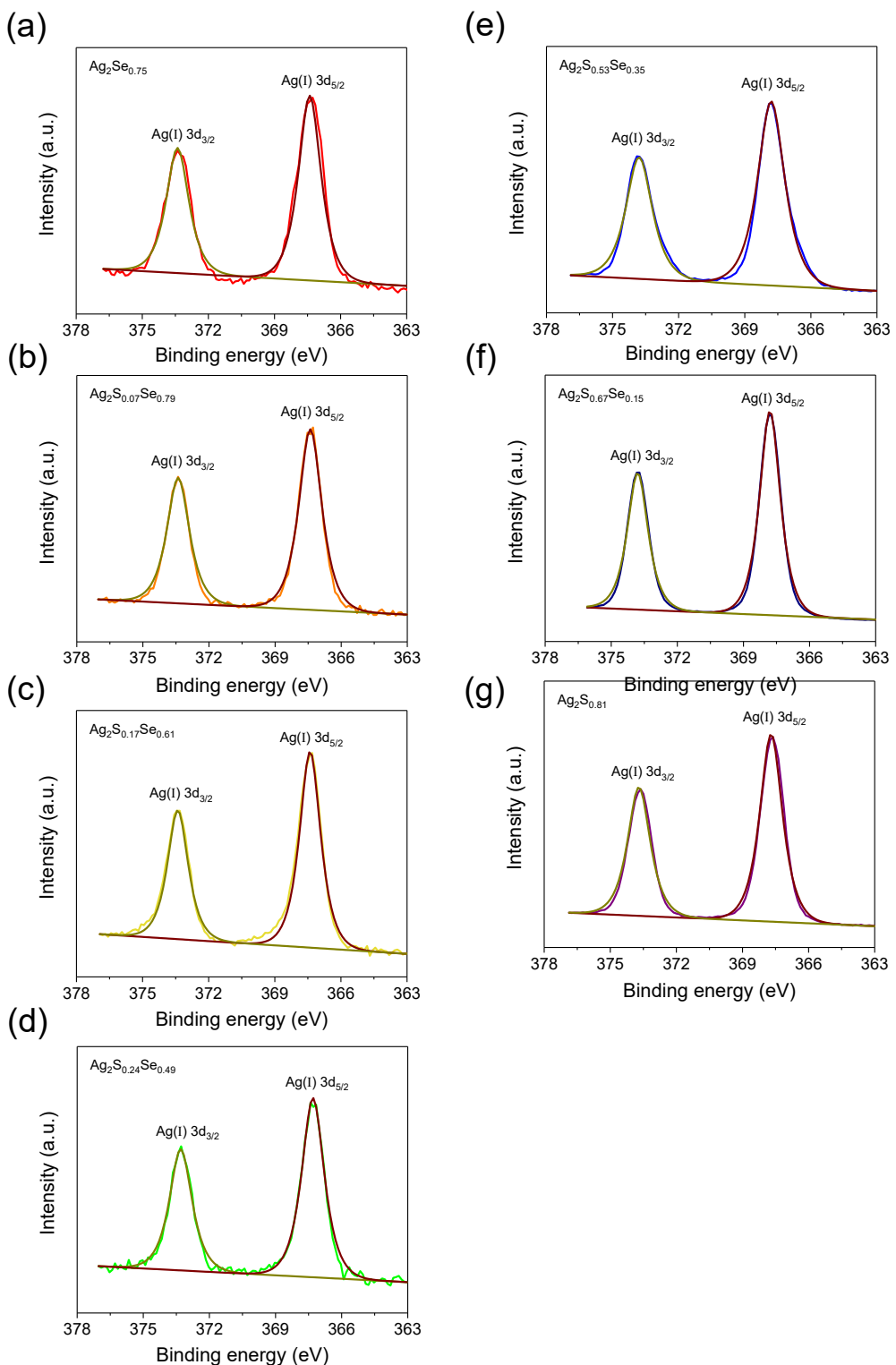


Fig. S5. The fitting results of XPS spectra of Ag 3d region of the various $\text{Ag}_2\text{S}_x\text{Se}_y$ nanocrystals.

Table S2. The peak locations of XPS spectra (Se 3p, S 2p, and Ag 3d) of the various $\text{Ag}_2\text{S}_x\text{Se}_y$ nanocrystals.

	$\text{Ag}_2\text{Se}_{0.75}$	$\text{Ag}_2\text{S}_{0.07}\text{Se}_{0.79}$	$\text{Ag}_2\text{S}_{0.17}\text{Se}_{0.6}$ 1	$\text{Ag}_2\text{S}_{0.24}\text{Se}_{0.49}$	$\text{Ag}_2\text{S}_{0.53}\text{Se}_{0.35}$	$\text{Ag}_2\text{S}_{0.67}\text{Se}_{0.1}$ 5	$\text{Ag}_2\text{S}_{0.81}$
Se 3p _{1/2} (eV)	165.3	165.3	165.4	165.4	165.3	165.4	-
Se 3p _{3/2} (eV)	159.4	159.5	159.4	159.5	159.5	159.5	-
S 2p _{1/2} (eV)	-	161.9	161.8	161.9	161.9	161.8	161.9
S 2p _{3/2} (eV)	-	160.9	160.8	160.9	160.9	160.8	160.8
Ag 3d _{3/2} (eV)	373.4	373.4	373.4	373.3	373.8	373.8	373.7
Ag 3d _{5/2} (eV)	367.4	367.4	367.4	367.3	367.8	367.8	367.7

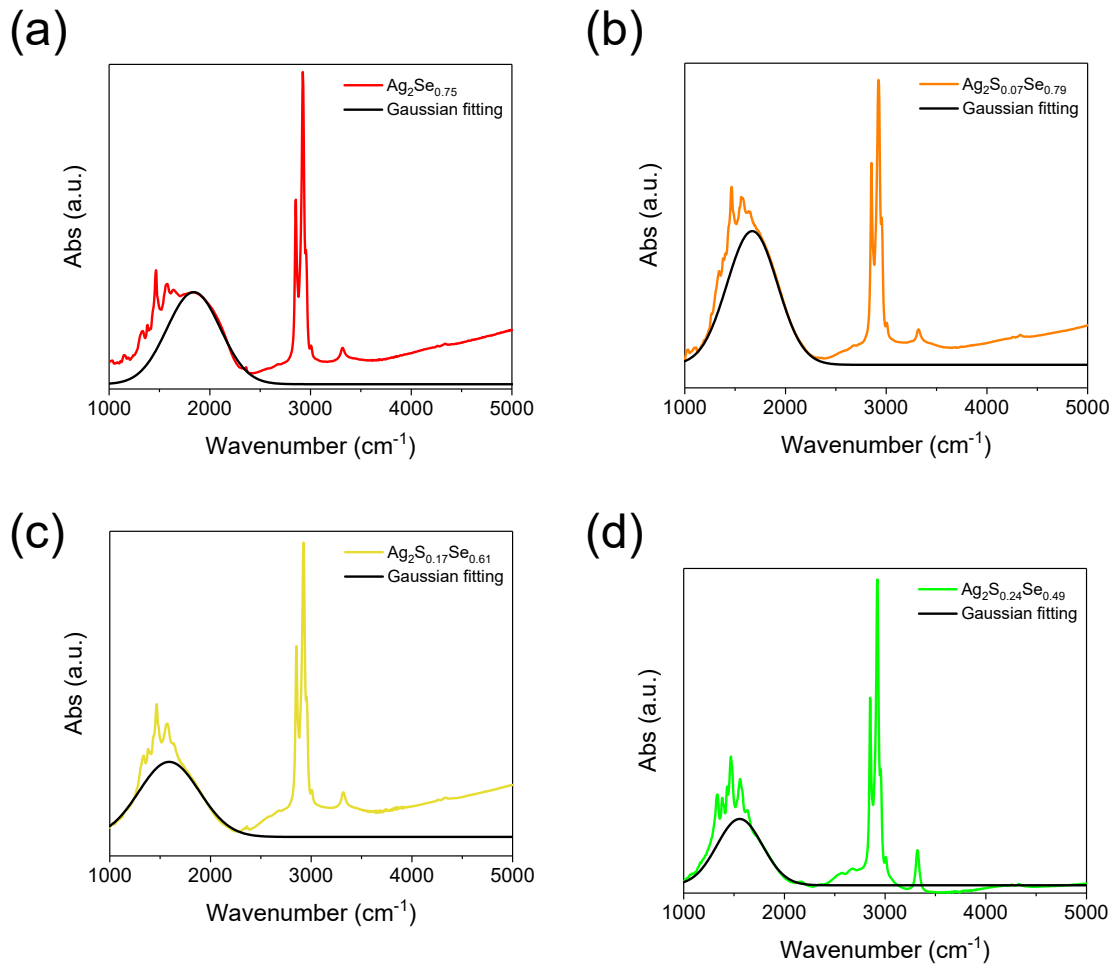


Fig. S6. The absorption spectra of the $\text{Ag}_2\text{S}_x\text{Se}_y$ nanocrystals fitted with Gaussian curves.

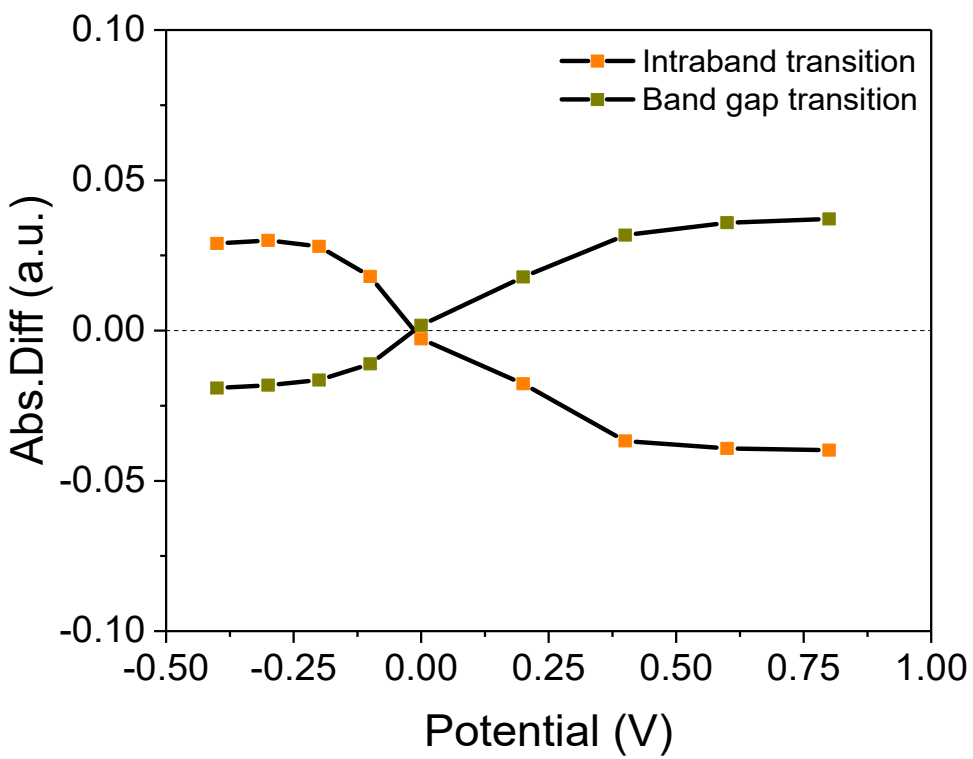


Fig. S7. The trends in the intraband and band gap transitions of the $\text{Ag}_2\text{S}_{0.23}\text{Se}_{0.51}$ nanocrystals at various SEC potentials.

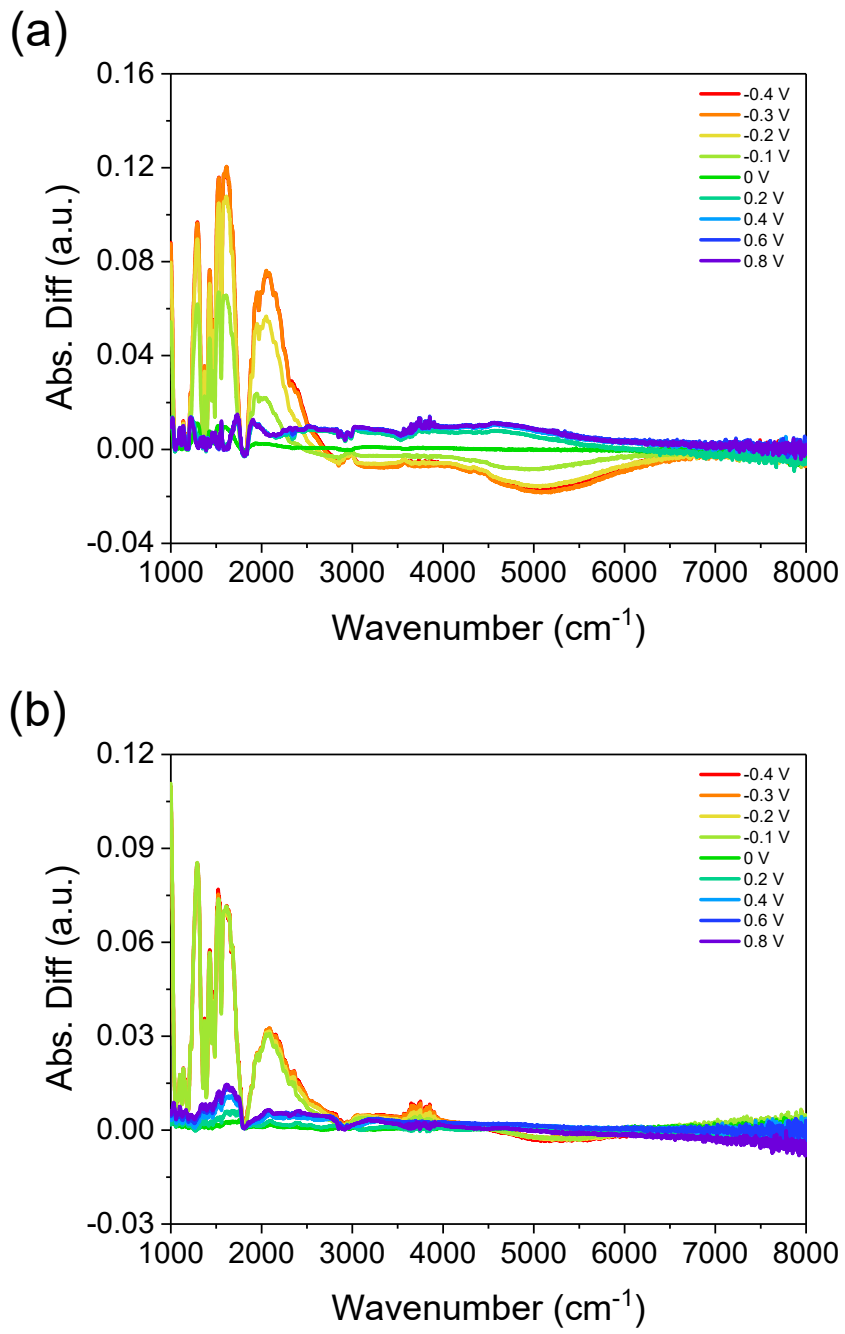


Fig. S8. The differential absorption spectra of (a) the $\text{Ag}_2\text{S}_{0.09}\text{Se}_{0.75}$ and (b) the $\text{Ag}_2\text{S}_{0.23}\text{Se}_{0.62}$ nanocrystals under various electrochemical potentials, as obtained from the SEC measurements.